

Physics 218c

Edges & Separatrix

Lecture 8a: Density Limit and Greenwald Scaling, SOL Width and Heatloads(Monday) 8b: Sheaths and P-W I (Tynan)→ All good things must come to an end- Monday is last class

- Still missing 6+ write-ups . . . !

→ Loose Ends- Rotation and Momentum Transport- for details on symmetry breaking, see P.D. Review 2013- for details on 'momentum pinch' see Ahmed, et. al. 107- for unifying Physical Picture, see Kosuga, P.D., Gursen and refs. therein (especially Ozawa)

approach is entropy production -
due Q_i, DT, ITG etc.

vs.

entropy destruction = Zonal flow and intrinsic rotation drive

⇒ Engine Paradigm ...

- for phenomenology OV, see review by Ida, Rice

- for the physics of boundary effects on intrinsic rotation, see ??

⇒ major issue | Most works (theory) have no-slip B.C.

LaBombard

⇒ Many papers posted.

Density limits RTE
why? high n $\rho = \frac{nm}{\Omega^2}$

Fueling → gas, pinch
 $r = -D_0 n + \gamma n$

Surprise < 0 $\frac{\gamma}{T_0}$

Greenwald → $\frac{I_p}{\pi a^2}$ → fundamental constraint

Stall - n limit $\frac{I_p}{\pi a^2}$
Carlos Hidalgo T3II n - limit → $\frac{I_p}{\pi a^2}$

Density Limits: Some Basic Aspects

- Not a review!
- Greenwald density limit:

$$\bar{n} = \bar{n}_g \sim \frac{I_p}{\pi a^2}$$



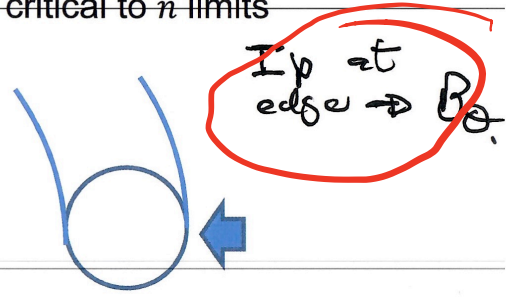
Constrains tokamak Operating Space

- Manifested on other devices
 - See especially RFP ($n \sim I_p$ scaling)

- Line averaged limit $\bar{n} \equiv$ line avg.
- (Too) simple dependence!?! widely upheld
- Begs origin of I_p scaling?! \rightarrow $\frac{1}{2}$

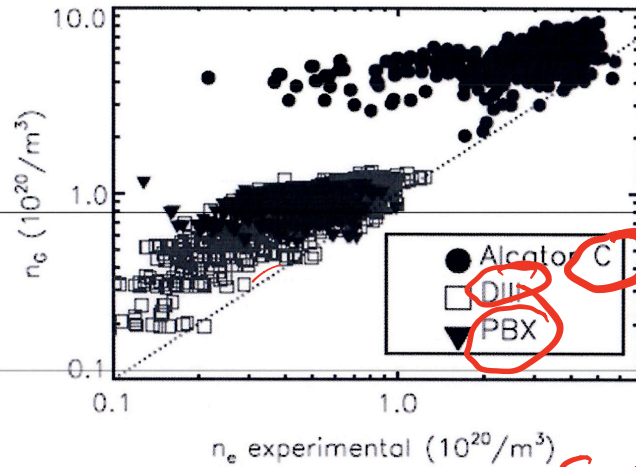
Stellarators?

- Most fueling via edge \rightarrow edge transport critical to \bar{n} limits



B_0
 \rightarrow $\frac{1}{2}$
 N.B. Physics of I_p scaling usually loosely linked to Z_{eff} !
 Z_{eff} screening length.

- Trends well established



walks

Greenwald ρ



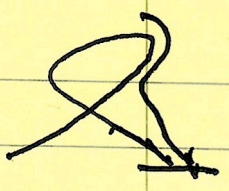
- Often (but not always!) linked to:

G. Field
Drake

- MARFE (radiative condensation instability) \leftrightarrow Impurity influx
 - MHD disruption
 - Divertor detachment \leftarrow
 - H \rightarrow L Back-transition
- radiation \rightarrow condensation \rightarrow cooling
 \rightarrow $DJ \uparrow$ \rightarrow Tearing \rightarrow Disruption

N.B. HDL (H-mode Density Limit) $\approx \bar{n}$
o/t back transition,
usually $\bar{n}_{HDL} \leq \bar{n}_G$.

Edge

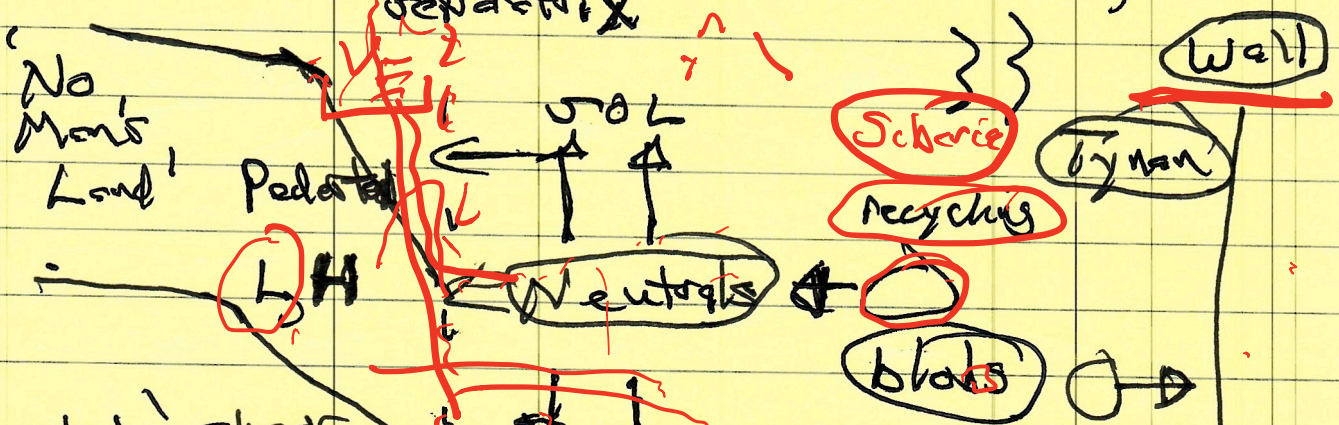
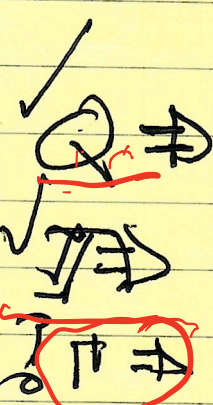


Cone \equiv closed field lines as discussed

What is the Edge?

JOL \equiv open field lines connect to limiter, plate

Cone

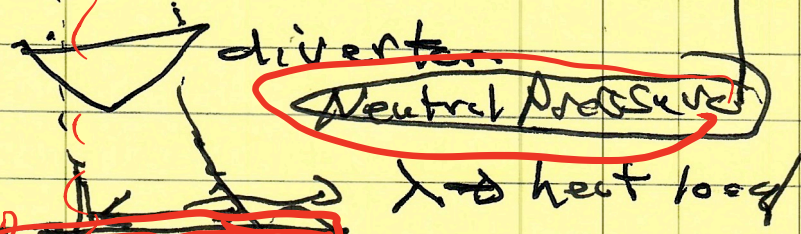


pedestal, shear layer at edge in L, H

Shear Layer

neutral penetration

$$T \sim e^{-x/\Delta}$$



in L mode, edge turbulence is strong

Plate PFC (Pur \rightarrow hole)

Sheath Tynan

$$\frac{e\phi}{T}, \frac{2kT}{eV} \gtrsim 1 \rightarrow 1$$
$$D, \chi$$

Drop in H-mode eV

isoly profile

Langmuir probes often used to study edge.

→ "Which" Edge? transition L→H

n_B ? → soft

β_{th}

L-mode

H-mode

Density Limit

Very strong turbulence

collapse of shear layer

$D_N \uparrow$

density outflow

Strong turbulence

Shear Layer

(Reynolds stress, Neoclassical)

High Transport

Pinch

Weak turbulence

Strong Shear

$(\partial v / \partial r) + \dots$

ELMs → MHD events (turbulence)

$D, \chi_i, \chi_e \downarrow, \chi_e \uparrow$

Pinch (β)

(don't take too far)

Order Parameter

$\beta \leftarrow$

$V_E / \Delta \omega_{UH}$

\rightarrow high

→ How determines E_r ?

→ Core → (closed)

$\nabla \cdot \mathbf{J} = 0$

with mainly

$\partial_r J_{\theta r} \approx 0$

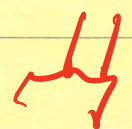
Radial force balance

→ $\partial L \rightarrow$ (open)

$\nabla \cdot \mathbf{J} = 0$ with

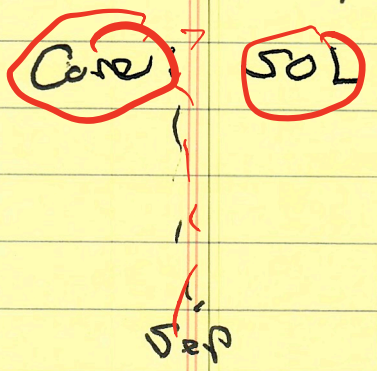
$\partial_r J_r + \partial_z J_z = C$

sheath b.c.

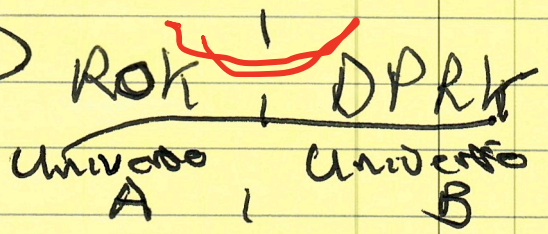


→ What about the edge?

- Stupidity \Rightarrow Core-SOL Boundary



What people think

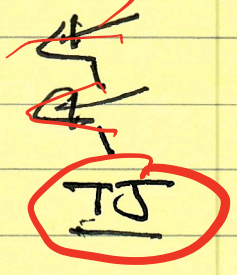
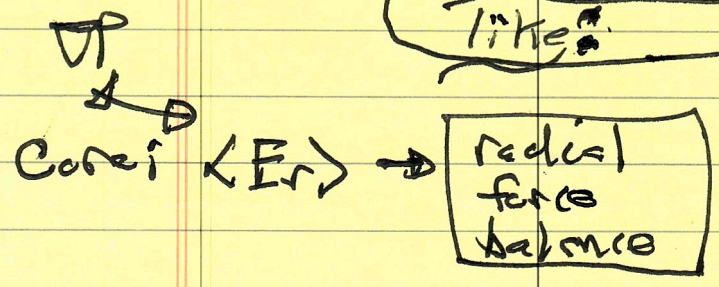
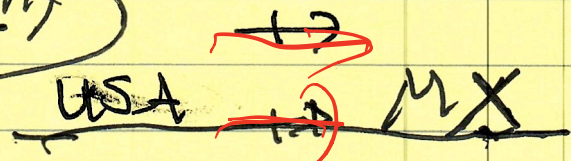


Key: transition layer.

How big - ρ_0 ?

38th Parallel

What its really like



Edge: $\langle E_r \rangle \rightarrow \langle \phi \rangle \rightarrow$ Sheath

$$\langle \phi \rangle \approx \frac{T}{|e|} \sim T e^{-x/\lambda} T_{sc0}$$

so

$$V_E' \approx \frac{T}{|e|} \lambda^2$$

SOL width

- In SOL

$$\nabla \cdot \mathbf{\Gamma} = 0 \Rightarrow \nabla_{\perp} \Gamma_{\perp} + \nabla_{\parallel} \Gamma_{\parallel} = 0$$

\downarrow
 parallel losses

In core

$$\nabla \cdot \mathbf{\Gamma} = 0$$

$\Rightarrow \Gamma = \text{const.}$ (fixed flux)

For Density Limit, first ask:

→ What of L-mode? → core state

- lots of info → Lyman- α probe (since Zeta → Robinson & Russett)

- intensities, direct measurement of fluxes → $\langle \tilde{v}_r \tilde{n} \rangle$, $\langle \tilde{v}_r \tilde{v}_{\theta} \rangle$ especially T horder ρ cross phase

- interestingly, frequently see: $\tilde{n}/n \approx \frac{|\epsilon| \phi^{\dagger}}{T}$ (but $\alpha < 1$?) non-adiabatic

→ Candidates → see Zoo

[CDW, [ITG [DM]
[DTEM, [RBM [CRGDT) continuous

continuous
" Drift Waves " , extended to hydrodynamic electron regime

$\frac{k_{\perp}^2 v_{th0}^2}{\omega \sqrt{L}}$
LI

doesn't matter ?

Non adiabatic behavior is not surprising → MHD-like candidates

- What does matter ? - Shear Layer

- L-mode ^{1990's} tokamak Stellarator edges support a

Shear layer

- universal

- Observed first TEXT - mid 80's

Exhibited effects on eddies, etc. linked to turbulence control. →

~~...~~ Ritz 1990

121

Evidence for Confinement Improvement by Velocity-Shear Suppression of Edge Turbulence

Ch. P. Ritz, H. Lin, T. L. Rhodes, and A. J. Wootton

Fusion Research Center, The University of Texas, Austin, Texas 78712
(Received 10 April 1990)

The electrostatic fluctuations are decorrelated in the region of a naturally occurring $E_r \times B$ velocity shear close to the outermost closed flux surface of regular Ohmic TEXT discharges. The concomitant local steepening of the density profile and suppression of the fluctuations are consistent with theoretical predictions. The high-confinement mode (H mode) found in other tokamaks shows in exaggerated form similar characteristics and could thus be related to the same mechanism leading to a locally improved confinement.

PACS numbers: 52.55.Fa, 52.25.Gj

Quantitative comparisons on the TEXT tokamak demonstrate that electrostatic fluctuations are a major cause of the anomalous particle and energy transport in Ohmic discharges as suggested previously by other experiments.^{2,3} In addition, a radial electric field E_r has been shown to modify the global confinement⁴ as well as the edge turbulence and electrostatic-fluctuation-induced transport.^{2,5} Most recently a series of experiments has been conducted on the Constant Current Tokamak (CCT) using a highly biased emissive electrode.⁶ The biasing triggered a transition to a regime with the characteristics of the high-confinement mode (H -mode regime first reported on ASDEX⁷), which is one of the most successful paths to improve the plasma confinement in tokamaks. Associated with the transition on CCT was a measured increase in E_r , and thus in the rotation velocity $v_E \equiv v_{E \times B}$. Such changes in E_r have also been observed on DIII-D, a large tokamak, at the transition to the H mode.⁸ Since the physics of H modes is not well understood, this is a motivation for further experimental studies.

The above experiments suggest that one possible mechanism for improved confinement is a change in the edge electric field, and concomitant change in the $E \times B$ rotation velocity v_E and the fluctuation levels. Theoretical work⁹⁻¹⁴ shows that, if changes in radial electric field result in an angular-velocity shear, then turbulence can be reduced leading to a decreased outward transport. In this paper we examine the theoretical predictions of turbulence suppression by sheared plasma rotation. Based on results from TEXT we demonstrate a clear correlation between velocity shear, reduction of the turbulence, and local improvement of the confinement.

A velocity shear due to a peaking plasma potential close to the outermost closed flux surface has been characterized on TEXT¹⁵ and other devices.^{16,17} The mean velocity of the fluctuations perpendicular to B measured with a two-point correlation technique in the laboratory frame of reference,

$$v_{ph} = \frac{\sum_{k>0, \omega} [\omega/k_\theta(\omega)] S(k, \omega)}{\sum_{k>0, \omega} S(k, \omega)},$$

is dominated by $v_E = E_r/B$ effects,¹⁸ as shown in Fig. 1(a), where v_{de} is the diamagnetic drift velocity. (The contribution to v_E from ∇p is thus small and only slowly varying with radius.) The density and floating potential fluctuations, \tilde{n} and $\tilde{\phi}$, are reduced in a region shifted to larger r/a from the shear region by roughly half the radial shear width, as shown in Fig. 1(b). The mean density is slightly steepened in the region of maximal shear, as

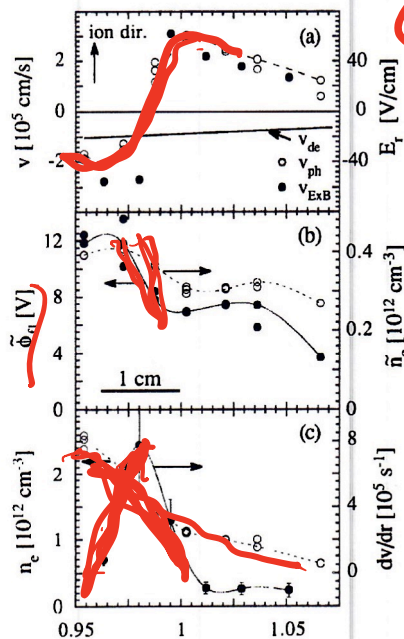


FIG. 1. Radial profiles for a discharge with $B_0 = 2$ T, plasma current of 200 kA, and chord-averaged density of $n_{chord} = 2 \times 10^{13} \text{ cm}^{-3}$. (a) Phase velocity of the fluctuations v_{ph} (closed circles), $v_{E \times B}$ plasma rotation (open circles), and drift velocity v_{de} . (b) Density and floating potential fluctuations. (c) Density and velocity shear. The statistical error for individual shots is of order the symbol size and shot-to-shot reproducibility is given by the individual symbols. The systematic error in the plasma position is 0.5 cm or $r/a = 0.02$.

shown in Fig. 1(c). The steepening is not pronounced, but consistently found on reproducible discharges.

The (one-point) correlation time τ_c^{lab} of the fluctuations measured in the laboratory frame of reference is obtained from the e -folding time τ of the autocorrelation function $R(\tau, r) \equiv \langle x(t, r)x(t + \tau, r) \rangle$. The fluctuation quantity $x(t, r)$ is the ion saturation current (proportional to density) and the angular brackets represent averaging over a temporal interval large compared to τ and ensemble averaging over several realizations. From Fig. 2 we find $\tau_c^{lab} = 10 \pm 1.5 \mu s$ behind the velocity shear ($r/a \approx 1$), $2 \pm 0.4 \mu s$ at the location of maximal shear, and $5 \pm 1 \mu s$ on the bulk plasma side of the shear layer ($r/a \approx 0.95$).

Similarly we compute the normalized cross-correlation function between two points r and $r + \delta r$.

$$\gamma(\tau, r, \delta r) \equiv C(\tau, r, \delta r) / [R(\tau = 0, r)R(\tau = 0, r + \delta r)]^{1/2},$$

where the cross-correlation function is

$$C(\tau, r, \delta r) \equiv \langle x(t, r)y(t + \tau, r + \delta r) \rangle.$$

By varying the Langmuir-probe separation δr we obtain the correlation lengths in the radial, poloidal, and toroidal directions from the separations for which the peak values of $\gamma(\tau, r, \delta r)$ decrease to $1/e$ of the values at $\delta r = 0$. The resulting correlation lengths on the bulk plasma side of the velocity shear ($r/a = 0.95$) are $\sigma_r \approx 0.5$ cm, $\sigma_\theta \approx 1$ cm, and $\sigma_\phi \approx 100$ -200 cm.¹⁹ To study the dependence of the correlation length on the velocity shear we measured the fluctuations simultaneously with an array of four probes separated poloidally and toroidally by a fixed distance of $\delta r = 3$ mm. As shown in Fig. 3 the peak values of the normalized cross-correlation function decrease in the shear layer with respect to the values on either side for both radially and poloidally separated probes. (The decrease is not large since the probe spacing is within a correlation length.) Furthermore, the τ dependences of $\gamma(\tau, r, \delta r)$ in the poloidal and radial directions are similar in the shear layer.

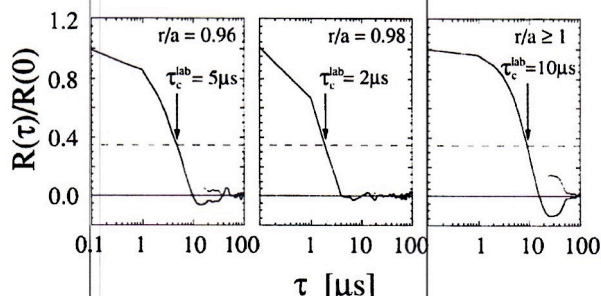


FIG. 2. Normalized one-point correlation function for two positions on either side of the shear layer and in the velocity shear. Dotted curve is the absolute value. Arrow indicates e -folding time τ_c^{lab} .

The turbulence is thus isotropic perpendicular to the magnetic-field direction, in contrast to the turbulence on either side of the shear layer where the decorrelation is faster in the radial direction than in the poloidal direction, consistent with the correlation-length measurements.

Relating the experimental observations to theoretical models, we can form three groups of questions: (i) What causes the peaking plasma potential leading to the strongly nonuniform electric field? (ii) Can the free energy in the velocity shear drive instabilities? (iii) Can the velocity shear suppress turbulence and thus improve the confinement? The first two questions are only briefly addressed for completeness.

On TEXT the width of the plasma potential peak which is connected with the velocity shear is typically 2 cm and thus approximately of the width of a poloidal ion Larmor radius (banana orbit width) for the hot-ion tail with $v^*(v) \leq 1$. The positive peak of the plasma potential causing the nonuniform radial electric field is thus possibly due to a differential orbit loss mechanism at the outermost closed flux surface.^{11,20,21} Mechanisms causing a nonambipolar transport may also generate such effects.

For the strong velocity shear measured here, the Kelvin-Helmholtz (KH) instabilities²² must be examined. The radial extent over which significant fluctuation levels are observed experimentally is much larger than the velocity-shear region. Further the fluctuation level is reduced and not enhanced in the velocity-shear region. Based on these experimental results, the KH instability is not expected to dominate the edge turbulence. A theoretical study also comes to the conclusion that the edge plasma of TEXT is KH stable because of the stabilizing role of the magnetic shear.⁹

Before the velocity shear is sufficient to destabilize KH instabilities it is already capable of reducing the ambient turbulence level due to the fissuring of fluid elements subject to a velocity shear.¹² A nonuniform radial electric field ($E_r' = \partial E_r / \partial r \neq 0$) causes in a slab a velocity dif-

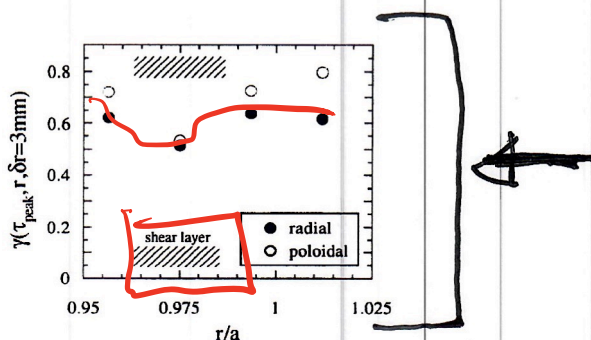


FIG. 3. Peak values of the normalized two-point correlation function for poloidally and radially separated probes with fixed separations of $\delta r = 3$ mm.

- L → H transition builds on base state of OH shear layer (Hickelgo)

- Shear Layer accountable from turbulent Reynolds stresses,

Shear layer
regulatory
L-mode

Now back to Density Limit

Shear
Layer
Collapse

- Edge particle transport crucial to density limit

d

- Greenwald small pellet relaxation

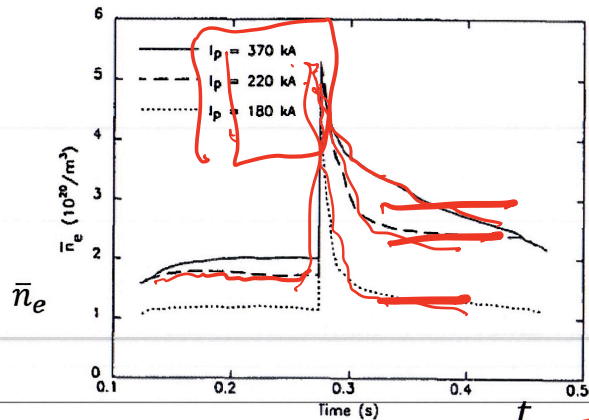
Perturbative Transport
Exit

⇒ Edge sheds excess density without disruption

88

⇒ Density limit linked to intrinsic physics of L-mode edge transport.

- Argue: Edge Particle Transport is crucial
 - ‘Disruptive’ scenarios secondary outcome, largely consequence of edge cooling, following fueling vs. increased particle transport
 - \bar{n}_g reflects fundamental limit imposed by particle transport
- A Classic Experiment (Greenwald, et. al.)



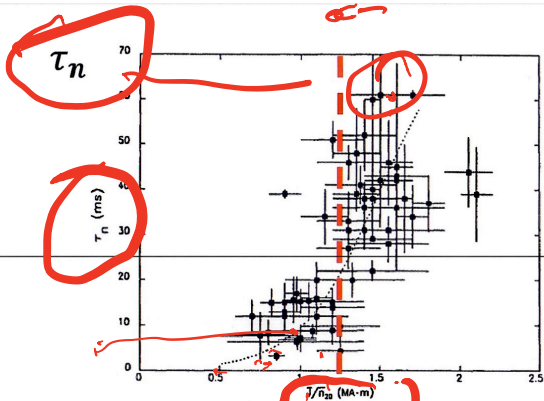
(Alcator C)

- Density decays without disruption after shallow pellet injection
- \bar{n} asymptote scales with I_p ←
- Density limit enforced by transport-induced relaxation
- Relaxation rate not studied (?)

TBD

15

• More Evidence for Role of Edge Transport

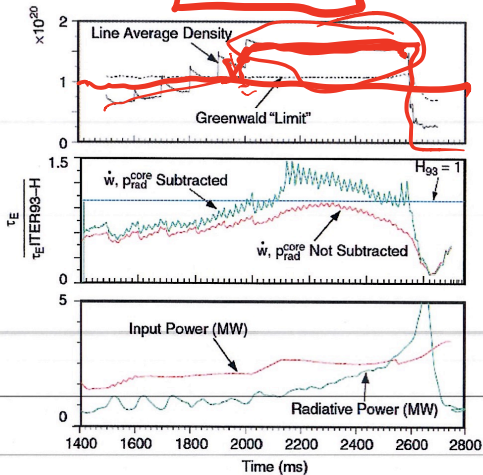


Pert.

- Post-pellet density decay time vs \bar{I}/\bar{n} .
- Increase in relaxation time near (usual) limit: $\bar{I}/\bar{n} \sim 1+$

C-Mod (Fluctuations?)

\bar{I}/\bar{n}

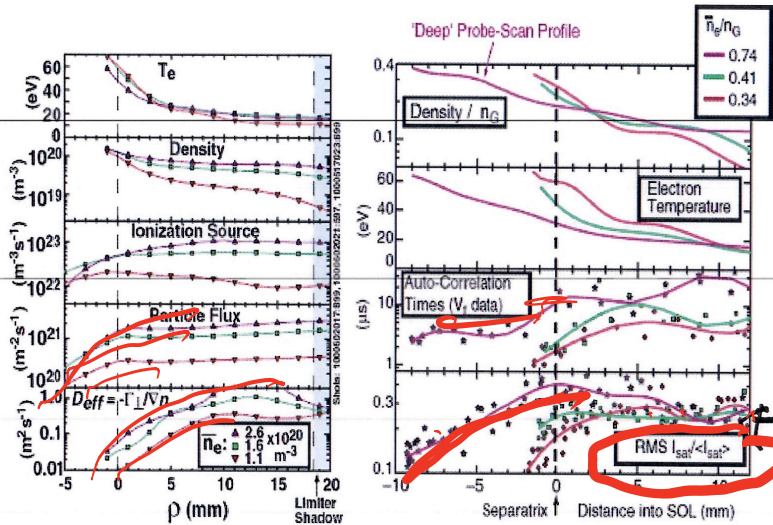


- Pellet in DIII-D beat \bar{n}_g
- Peaked profiles \leftrightarrow enhanced core particle confinement (ITG turbulence reduced?)
- Reduced particle transport \rightarrow impurity accumulation - issue with pellet.

(N.B. Deeper deposition)

advantage ELMy H-mode (grossy) Q/H

Density limit \leftrightarrow Fluctuation Structure



C-Mod profiles,
Greenwald et al, 2002, PoP

- Average plasma density increases as a result of edge fueling \rightarrow edge transport crucial to density limit.
- As n increases, high \perp transport region extends inward and fluctuation activity increases.
- Turbulence levels increase and perpendicular particle transport increases as $n/n_G \rightarrow 1$.

Why?

N.B. Increase in D_{\perp} relative to χ_{\perp} (N.B. high n , $\chi_{\perp} \sim 1/n$) \Rightarrow detachment!

Greenwald Review

Edge cooling

Core cooling

Flux trapped

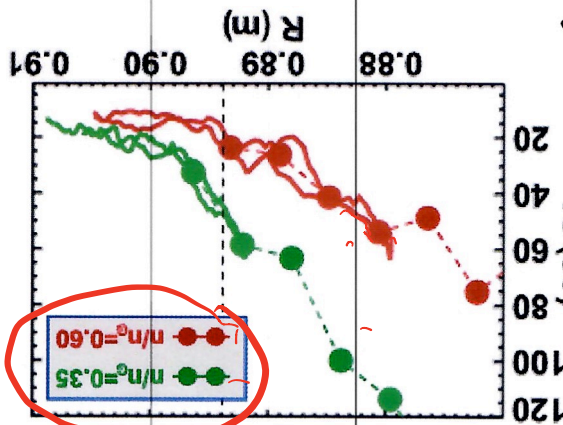
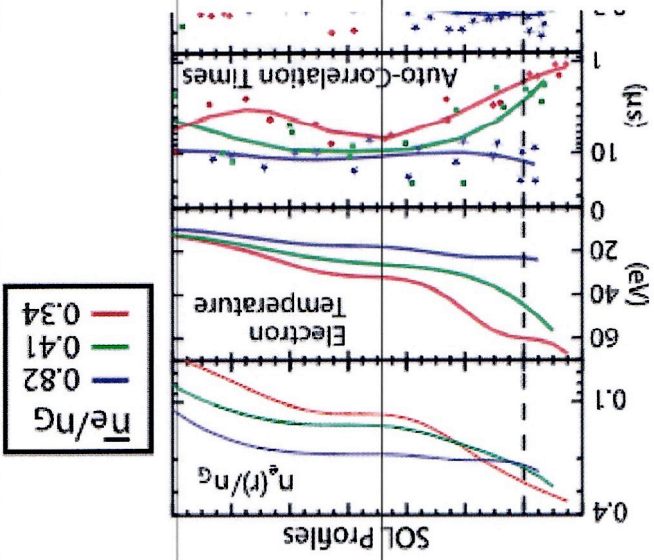


FIG. 17. Edge temperature profiles show the progressive edge cooling as the normalized density is increased toward n_g.

down at the end of a plasma shot is often at the rate required to stay just below the density limit.⁵ That is, the discharge sheds particles during ramp-down to keep n/n_g just below 1. C-Mod carried out experiments to measure the change in edge temperature along with any changes in fluctuations that accompany the approach to the density limit.^{87,104} Well before the limit was reached, changes in the time-averaged SOL density profiles were observed, with progressive increases in the far-SOL density and overall flattening of the profiles even with modest increases in the separatrix density as shown in Fig. 9. At the same time, the amplitude, frequency, and velocity of blob production increased.^{103,108} This picture is supported by fluid models, which predict very strong transport under these conditions.^{90,109} At still higher densities, the boundary between the near-SOL and far-SOL moved inward, with the region of colder plasma, intermittent fluctuations and blob creation¹¹⁰ eventually crossing the separatrix and intruding onto regions of closed field lines as



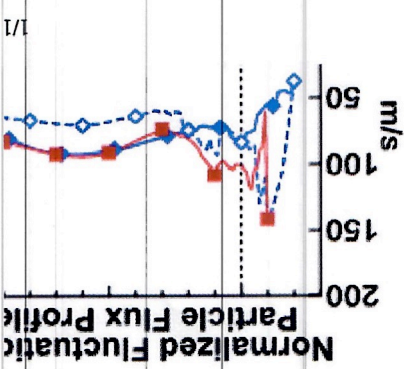
Legend for Figure 18:

- n/n_g = 0.34 (Red line)
- n/n_g = 0.41 (Green line)
- n/n_g = 0.82 (Blue line)

2. Poloidally asymmetric transport flows

An important prediction of turbulence transport would have a significant ball is, the turbulence would be stronger (LFS) of the plasma, which has a bad curvature the high-field side (HFS) with its good scanning probe, mounted on the inner wall tokamak's strong toroidal field cross-section small coil in the probe mechanism.^{97,111} the more remarkable in requiring that t

seen in Figs. 17 and 18. The net cooling exchange between warm plasma convection reaches roughly to the position of 0.8 movement of about 3 cm on C-Mod), a motion is triggered. As the density limit is given the low upstream temperatures, transport channel is starved. This contrast at lower density where all power is lost to the divertor. In that case, the upstream boundary between open and closed the close to the limit, perpendicular transport open field lines and the temperatures values. The appearance of Marfes or divertor then inevitable—if the plasma has not sites, it will certainly detach near the no power is available in the parallel observations coupled to the predictions make a compelling case for turbulence cause of the density limit, work remains change in the equilibrium temperature. is raised, which will require, at a minimum to equations for turbulence and transport coupled to a neutral transport



Top

18

→ Why does the particle transport increase as $\Lambda \rightarrow \Lambda_E$?

→ If V_E' regulates transport → look at the shear layer

→ Shear Layer collapse scenario.

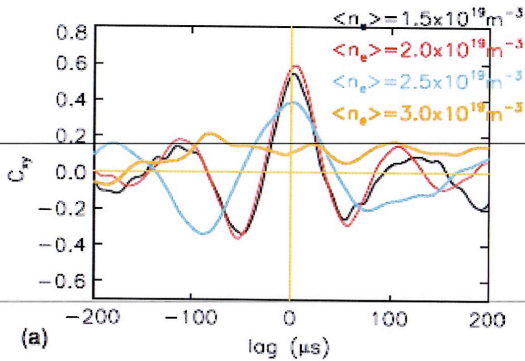
Recent Experiments - 1



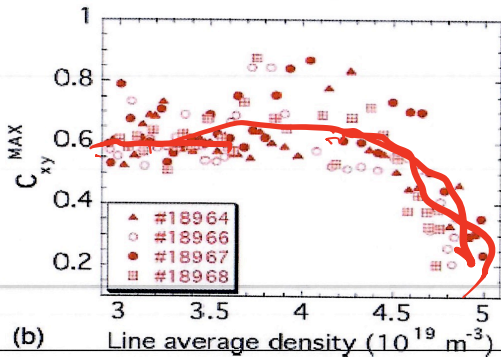
(Y. Xu et al., NF, 2011)

LRC vs \bar{n}

LRC \rightarrow Long range correlation
 \rightarrow ZF!



- Decrease in maximum correlation value of LRC (i.e. ZF strength) as line averaged density n increases at the edge ($r/a=0.95$) in both TEXTOR and TJ-II.
- At high density ($\langle n_e \rangle > 2 \times 10^{19} \text{ m}^{-3}$), the LRC (also associated with GAMs) drops rapidly with increasing density.
- The reduction in LRC due to increasing density is also accompanied by a reduction in edge mean radial electric field (Relation to ZFs).



Is density limit related to edge shear decay?

See also M. Pedrosa 2007
C. Hidalgo 2006.

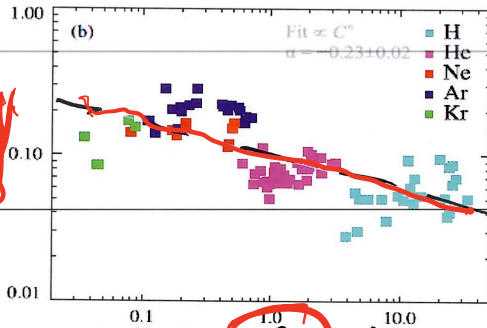
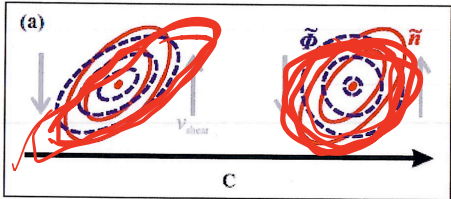
TJ II

Recent Experiments - 2

Eddy Tilt

(Schmid, Mans et al., PRL, 2017) – stellarator experiment

(not in density limit exp.)



- Experimental verification of the importance of **collisionality** for large-scale structure formation in TJ-K.
- Analysis of the Reynolds stress shows a decrease in coupling between density and potential for increasing collisionality → **hinders zonal flow drive** (Bispectral study)
collisionality ∝ density
- **Decrease of the zonal flow contribution to the total turbulent spectrum with collisionality C.**

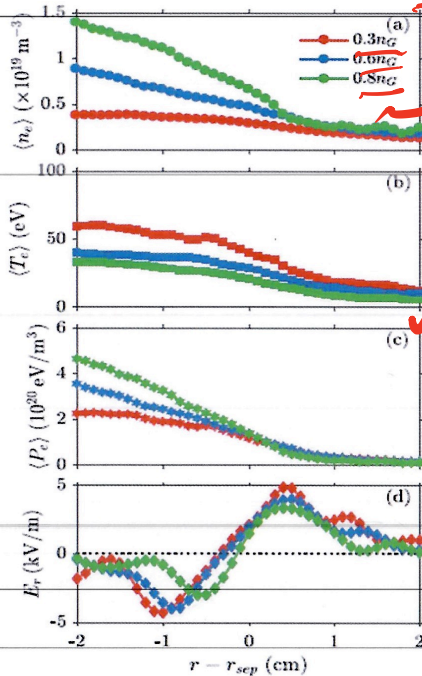
- Increase in decoupling between density (red) and potential (blue) coupling with collisionality C.
- Increase in ZF contribution to the spectrum in the adiabatic limit ($C \rightarrow 0$)

$C \Leftrightarrow$ adiabaticity $k_{\parallel}^2 V_{th}^2 / \omega v$

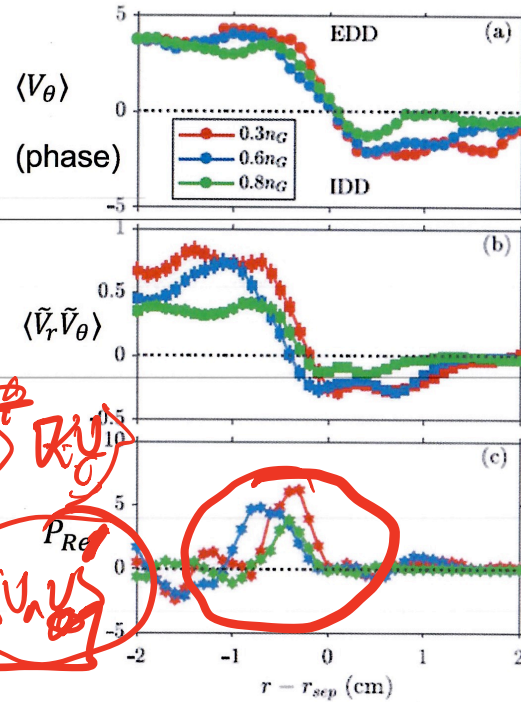
Basic Results

- OH, $I_p \sim 150\text{kA}$, $B_T = 1.3\text{T}$, $q = 3.5 \rightarrow 4$
- $\bar{n} = 0.25 \rightarrow 0.9 \bar{n}_g$
- Profiles

- Fluctuation Properties



HL-2A

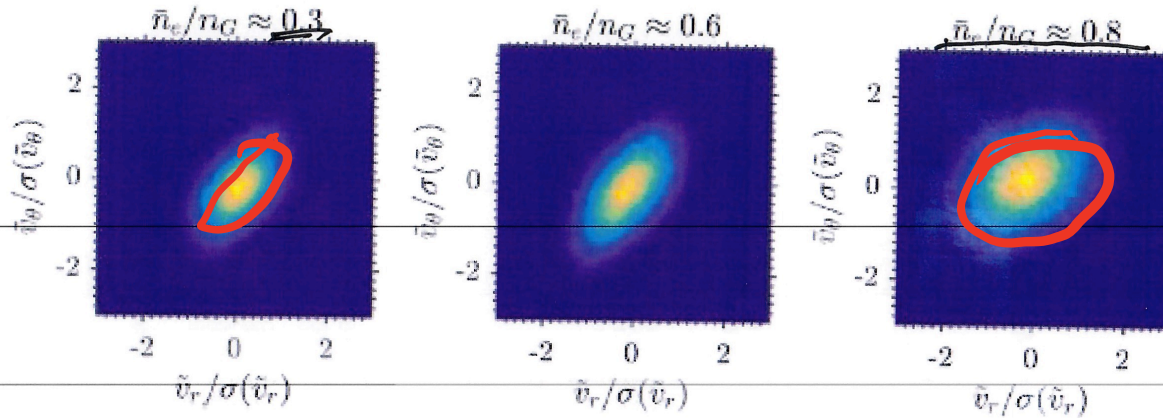


$\langle V_\theta \rangle$
 $\langle \tilde{V}_r \tilde{V}_\theta \rangle$
 P_{Re}

$$P_{Re} = -\langle V_\theta \rangle \partial_r \langle \tilde{V}_r \tilde{V}_\theta \rangle \rightarrow \text{energy gained by low-f flow}$$

DROPS as $\bar{n} \rightarrow \bar{n}_g$

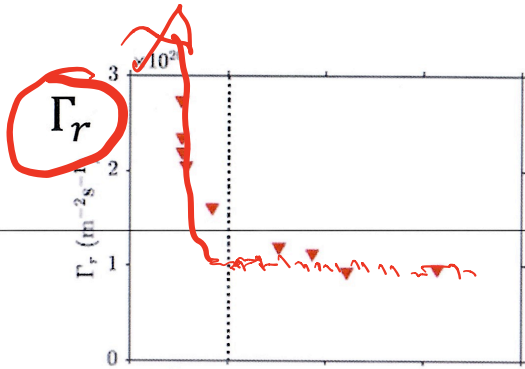
Recent Studies, Hong, et. al. (NF 2018)



- Joint pdf of $\tilde{V}_r, \tilde{V}_\theta$ for 3 densities, $\bar{n} \rightarrow n_g$
- $r - r_{sep} = -1cm$
- Note:
 - Tilt lost, symmetry restored as $\bar{n} \rightarrow \bar{n}_g$
 - Consistent with drop in P_{Re}

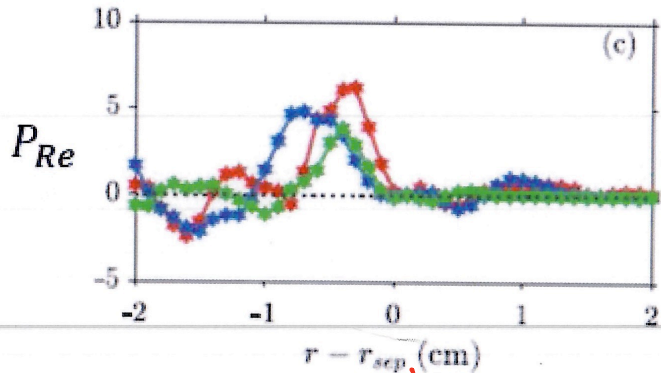
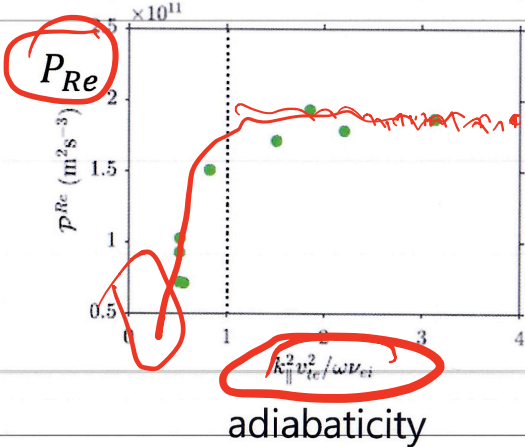
→ Weakened shear flow
production by Reynolds stress

Key Parameter: Electron Adiabaticity



- Electron adiabaticity $\alpha = \frac{k_{||}^2 v_{th}^2}{|\omega| v_{ei}}$ emerges as interesting local parameter. $\alpha \sim 3 \rightarrow 0.5$ during \bar{n} scan!

- Particle flux \uparrow and Reynolds power $P_{Re} = -\langle V_{\theta} \rangle \partial_r \langle \tilde{V}_r \tilde{V}_{\theta} \rangle \downarrow$ as α drops below unity.



N.B. Plasma beta remained very low

\rightarrow kills the RBM scenario

RBIM

$\beta \sim (n/n_0)^2$

Synthesis of the Experiments

- Shear layer collapse and turbulence and D (particle transport) rise as $\frac{\bar{n}}{\bar{n}_G} \rightarrow 1$.
→ Key microphysics of density limit !?
- ZF collapse as $\alpha = \frac{k_{\parallel} v_{th}^2}{|\omega| \nu}$ drops from $\alpha > 1$ to $\alpha < 1$. (or via ZF damping)
→ Effect on production
- Degradation in particle confinement at density limit in L-mode is due to breakdown of self-regulation by zonal flow
- Note that β in these experiments is too small for conventional Resistive Ballooning Modes (RBM) explanation.

→ How reconcile all these with our understanding of drift wave-zonal flow physics?

The Key Questions

- What physics governs shear layer collapse (or maintenance) at high density?

⇔ 'Inverse process' of familiar $L \rightarrow H$ transition !?

i.e. $L \rightarrow H$: $\begin{cases} \text{shear layer} \rightarrow \text{barrier} \\ \text{turbulence} \end{cases}$

Density Limit: $\begin{cases} \text{strong} \\ \text{turbulence} \end{cases} \leftarrow \begin{cases} \text{shear layer,} \\ \text{turbulence} \end{cases}$

→ In particular, what is the fate of shear flow for

hydrodynamic electrons: $k_{\parallel}^2 V_{th}^2 / \omega v < 1$?

More generally → strong collisionality .

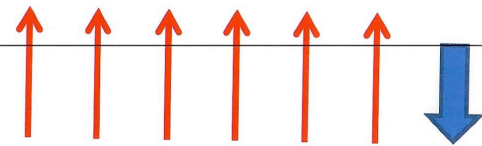
Advertisement: Singh P.R., NFI



Step Back: Zonal Flows Ubiquitous! Why?

- Direct proportionality of wave group velocity and wave energy density flux to Reynolds stress \leftrightarrow spectral correlation $\langle k_x k_y \rangle$

Causality \leftrightarrow Eddy Tilting



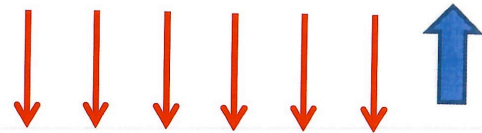
$\omega_k = -\beta k_x / k_{\perp}^2$: (Rossby)



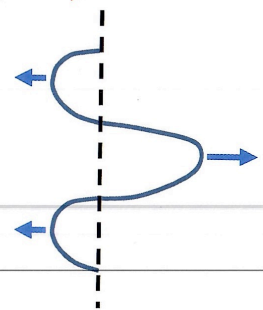
$\rightarrow V_{g,y} = 2\beta k_x k_y / (k_{\perp}^2)^2$

$\rightarrow \langle \tilde{v}_y \tilde{v}_x \rangle = -\sum_k k_x k_y |\phi_k|^2$

same



So: $V_g > 0$ ($\beta > 0$) $\leftrightarrow k_x k_y > 0 \rightarrow \langle \tilde{v}_y \tilde{v}_x \rangle < 0$



- Outgoing waves generate a flow convergence! \rightarrow Shear layer spin-up

But NOT for hydro convective cells:

- $\omega_r = \left[\frac{|\omega_{*e}| \hat{\alpha}}{2k_{\perp}^2 \rho_s^2} \right]^{1/2} \rightarrow$ for convective cell of H-W
- $V_{gr} = -\frac{2k_r \rho_s^2}{k_{\perp}^2 \rho_s^2} \omega_r \quad \leftarrow ?? \rightarrow \quad \langle \tilde{V}_r \tilde{V}_{\theta} \rangle = -\langle k_r k_{\theta} \rangle;$ direct link broken!

→ Energy flux NOT simply proportional to Momentum flux →



→ Eddy tilting ($\langle k_r k_{\theta} \rangle$) does not arise as direct consequence of causality

→ ZF generation not 'natural' outcome in hydro regime!] ←

→ Physical picture of shear flow collapse emerges

Dispersion Relation for $\alpha < 1$ and $\alpha > 1$

Dispersion relation:
$$\omega = \frac{1}{2} \left(-i \frac{\hat{\alpha}(1 + k_{\perp}^2 \rho_s^2)}{k_{\perp}^2 \rho_s^2} + \sqrt{\frac{4i\omega^* \hat{\alpha}}{k_{\perp}^2 \rho_s^2} - \left(\frac{\hat{\alpha}(1 + k_{\perp}^2 \rho_s^2)}{k_{\perp}^2 \rho_s^2} \right)^2} \right)$$

$$\hat{\alpha} = -\frac{v_{th}^2}{v_{ei}} \nabla_{\parallel}^2$$

$$\alpha = \frac{k_{\parallel}^2 V_{the}^2}{v_{ei} |\omega|}$$

Adiabatic Limit:
($\alpha \gg 1$ and $\hat{\alpha} \gg |\omega|$)

$$\omega_{adiabatic} = \frac{\omega^*}{1 + k_{\perp}^2 \rho_s^2} + i \frac{\omega^{*2} k_{\perp}^2 \rho_s^2}{\hat{\alpha}}$$

Wave + inverse dispersion

(Classic Drift Wave)

Hydro Limit:
($\alpha \ll 1$ and $\hat{\alpha} \ll |\omega|$)

$$\omega_{hydrodynamic} \simeq \sqrt{\frac{\omega^* \hat{\alpha}}{2k_{\perp}^2 \rho_s^2}} (1 + i)$$

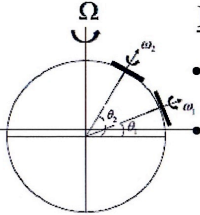
Convective Cell

key: $\alpha < 1 \rightarrow$ drift wave converts to convective cell

ZF Collapse \leftrightarrow PV Conservation and PV Mixing?

Back to
to the start.

How reconcile?

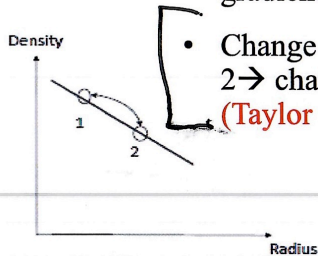


Rossby waves:

- $PV = \nabla^2 \phi + \beta y$ is conserved from θ_1 to θ_2 .
- Total vorticity $2\vec{\Omega} + \vec{\omega}$ frozen in \rightarrow Change in mean vorticity Ω leads to change in local vorticity $\omega \rightarrow$ **Flow generation (Taylor's ID)**

Drift waves:

- In HW, $q = \ln n - \nabla^2 \phi = \ln n_0 + h + \tilde{\phi} - \nabla^2 \phi$ conserved along the line of density gradient.
- Change in density from position 1 to position 2 \rightarrow change in vorticity \rightarrow **Flow generation (Taylor ID)**



Quantitatively

- Total PV flux $\Gamma_q = \langle \tilde{v}_x h \rangle - \rho_s^2 \langle \tilde{v}_x \nabla^2 \phi \rangle$
- Adiabatic limit $\alpha \gg 1$:
+ Particle flux and vorticity flux are tightly coupled (both prop. to $1/\alpha$)
- Hydrodynamic limit $\alpha \ll 1$:
- Particle flux proportional to $1/\sqrt{\alpha}$.
- Residual vorticity flux proportional to $\sqrt{\alpha}$.
- **PV mixing still possible without ZF formation \rightarrow Particles carry PV flux**

- **Branching ratio changes with α !**

\downarrow
Flow, Fluxes

The rest - Ongoing - - - -

HDL

→ SOL watch

Le Bonnard

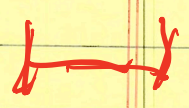
$$\lambda \sim \frac{1}{B_0}$$

→ Goldston $\frac{1}{2}$

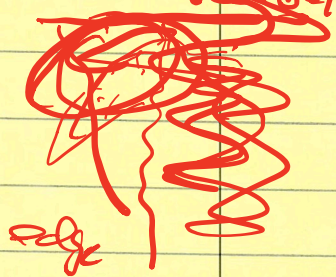
$$\lambda \sim \frac{v_{D, \perp} \sqrt{1 + \frac{v_{D, \perp}^2}{v_{th}^2}}}{R} \sim \frac{v_{D, \perp} \sqrt{1 + \frac{v_{D, \perp}^2}{v_{th}^2}}}{R} \sim \frac{v_{D, \perp} \sqrt{1 + \frac{v_{D, \perp}^2}{v_{th}^2}}}{R}$$

$$\lambda \sim \frac{v_{D, \perp}}{R} \sim \frac{v_{D, \perp}}{R}$$

SOL



turbulence



HDL →

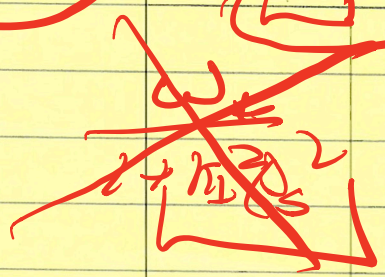
onset of SOL turbulence high?

HDL

Task Spreading

$$\langle \tilde{u}_r \tilde{u}_\theta \rangle \sim \frac{v_{D, \perp}}{R} \sim \frac{v_{D, \perp}^2}{R} + \frac{v_{D, \perp}^2}{R}$$

$\alpha \langle \tilde{u}_r \tilde{u}_\theta \rangle$



$$\omega_r \sim \omega_{D, \perp}$$